INL/RPT-22-68896
Revision 0

Single-Bar SMT Creep-Fatigue Testing on Alloy 617 with Software Controls on Elastic Follow-Up Feedback in Support of New Creep-Fatigue Design Methodology

September 2022

Heramb Mahajan
Idaho National Laboratory

Michael D. McMurtrey
Idaho National Laboratory

INL is a U.S. Department of Energy National Laboratory
operated by Battelle Energy Alliance, LLC

INL/RPT-22-68896
Revision 0

Single-Bar SMT Creep-Fatigue Testing on Alloy 617 with Software Controls on elastic Follow-Up Feedback in Support of New Creep-Fatigue Design Methodology

Heramb Mahajan
Idaho National Laboratory
Michael D. McMurtrey
Idaho National Laboratory

September 2022

Idaho National Laboratory
Advanced Reactor Technologies
Idaho Falls, Idaho 83415

http://www.art.inl.gov

Prepared for the
U.S. Department of Energy
Office of Nuclear Energy
Under DOE Idaho Operations Office
Contract DE-AC07-05ID14517

Page intentionally left blank

INL ART Program

Single-Bar SMT Creep-Fatigue Testing on Alloy 617 with Software Controls on elastic Follow-Up

INL/RPT-22-68896
Revision 0

September 2022

Technical Reviewer: (Confirmation of mathematical accuracy, and correctness of data and appropriateness of assumptions.)

Michael Heighes — September 8, 2022

Michael Heighes
Research Engineer

Date

Approved by:

Ting-Leung Sham — September 7, 2022

Ting-Leung Sham
NST Directorate Fellow

Date

M. Davenport — 9/7/2022

Michael E. Davenport
ART Project Manager

Date

Michelle Sharp — 9/7/2022

Michelle T. Sharp
INL Quality Assurance

Date

ABSTRACT

The Simplified Model Test (SMT) is an alternative way to calculate the creep-fatigue damage of elevated temperature components. The SMT approach unifies the creep and fatigue damage, simplifying the damage calculation process with improved accuracy. Traditionally, SMT tests have been conducted through the two bars: first is the driver bar and second is the test bar. The driver bar stays elastic and imposes the confinement to the second bar. This experimental procedure requires two test frames and a large test specimen, which limits the test parameter range and accessibility of this testing procedure. Hence, a single-bar SMT (SB-SMT) test has been developed to simplify complexity in SMT experiment setup. The software-controlled SB-SMT test process introduced completely replaces the driver bar. This paper discusses the SB-SMT test procedure with software controls. The challenges and critical parameters in the software-controlled SB-SMT procedure are addressed and recommendations are provided. A scoping test with a set of wider strain range, elastic follow-ups, and dwell time validate the proposed test procedure.

Page intentionally left blank

ACKNOWLEDGEMENTS

This research was sponsored by the United States (U.S.) Department of Energy (DOE) under Contract No. DE-AC07-05ID14517 with Idaho National Laboratory (INL), which is managed and operated by Battelle Energy Alliance. Programmatic direction was provided by the Office of Nuclear Reactor Deployment of the DOE Office of Nuclear Energy.

The authors gratefully acknowledge the support provided by Sue Lesica, Federal Lead for Advanced Materials, Advanced Reactor Technologies (ART) Program; Gerhard Strydom, INL, National Technical Director, ART Gas Cooled Reactors (GCR) Campaign; and Ting-Leung Sham, INL, ART Advanced Materials Technology Area Lead.

The authors also thank Joel A. Simpson of INL for his assistance in performing this work.

Page intentionally left blank

CONTENTS

FIGURES

TABLES

Page intentionally left blank

ACRONYMS

ART	Advanced Reactor Technologies
INL	Idaho National Laboratory
NEML	Nuclear Engineering Material Library
ORNL	Oak Ridge National Laboratory
SMT	Simplified Model Test
SB-SMT	Single-Bar Simplified Model Test

Page intentionally left blank

Single-Bar SMT Creep-Fatigue Testing on Alloy 617 with Software Controls on Elastic Follow-Up Feedback in Support of New Creep-Fatigue Design Methodology

1. MOTIVATION

Elevated temperature components experience cyclic loading which results in creep-fatigue damage. Traditionally, creep and fatigue damages are calculated separately, and evaluated against the creep-fatigue interaction diagram (ASME, 2021). This approach fails to accurately capture the material creep-fatigue interaction and results in a highly conservative design. An alternative creep-fatigue damage calculation method is under development that uses a Simplified Model Test (SMT) to unify the creep and fatigue damage (Jetter et al., 2016) calculations and compare it against the SMT design curves (Barua et al., 2020 and Barua et al., 2021). SMT can also capture the material behavior near notches and stress raisers. These SMT features estimate creep-fatigue material response accurately which results better life prediction of elevated temperature components.

The SMT design curves development needs SMT experiments that will cover a wide range of loading parameters. Conducting SMT experiments has many challenges. Traditional SMT experiments involve a two-bar approach, which requires a very large specimen and two servo-hydraulic systems (Wang et al., 2015, Wang et al. 2018). This approach is not efficient and has limitations on test parameters. There has been development toward a single-bar SMT (SB-SMT) approach, which addresses challenges in the traditional SMT procedure. Recent work at Oak Ridge National Laboratory (ORNL) has established the SB-SMT procedure which simplifies the SMT procedure (Wang et al. 2018, Wang et al. 2019a, Wang et al. 2019b). This work replaces the driver bar with an electronic spring which amplifies recorded strain value based on force relaxation in the previous time step, and applies the amplified strain value in the next time step. Although this procedure simplifies the traditional SMT procedure, a high signal-to-noise ratio is needed to get useful data. Hence, there is a need for an efficient and accurate SB-SMT procedure.

The software-controlled SB-SMT was developed at Idaho National Laboratory (INL), which controls the test through software inputs and internal variables (McMurtrey and Simpson, 2020). This report addresses challenges in the software-controlled SB-SMT approach and presents analytical methods to estimate the SB-SMT test parameters for desired strain range and elastic follow-ups. A scoping test on Alloy 617 at 950℃ validates the proposed software-controlled SB-SMT procedure.

2. BACKGROUND

At elevated temperature, enhanced creep damage is observed in stressed regions when elastically loaded regions of components act like an elastic spring, imposing additional stresses on already heavily loaded regions (Roche, 1981). This enhanced creep damage mechanism in stressed regions is referred to as an 'elastic follow-up' effect. Typical components in advanced reactors have geometric discontinuities and elastic follow-ups. During reactor operations, these components go through cyclic loads at elevated temperature, resulting into material degradation due to creep-fatigue damage. Current damage analysis and design methodology calculates creep and fatigue damage separately, then the calculations are evaluated against the creep-fatigue interaction diagram, also known as D-diagram. This approach fails to capture the accurate elastic follow-up influence and creep-fatigue interaction in materials resulting in a highly conservative design. To address the issue of over-conservatism in creep-fatigue analyses, integrated Elastic-Perfectly Plastic Simplified Model Test (EPP-SMT) methodology was investigated. The EPP-SMT method uses coupled creep-fatigue damage calculation, eliminating the need for D-diagram. The EPP-SMT approach considers actual component interaction during analysis and calculates the creep-fatigue damage accurately for a given component. This capability makes EPP-SMT an attractive approach for analysis and design for advanced reactor components.

A schematic of components with geometric discontinuity and elastic follow-up is shown as two bars in Figure 1a. External displacement is applied on the system, such that the larger bar remains elastic. During dwell time, the small bar experiences stress relaxation due to elastic follow-up from the large bar. This is the global elastic follow-up represented by q_n. The geometric discontinuity at the notch or sharp corner between the two bars results in stress concentration. Stress redistribution occurs near geometric discontinuity during dwell time. This stress redistribution results in local elastic follow-up indicated by q_L. The two-bar problem can be modified to a four-bar problem as shown in Figure 1b. Members 3 and 4 capture the global scale component characteristics and interactions. Members 1 and 2 indicate local scale behavior such as stress concentration and redistribution near stress raisers. The global level elastic follow-up (q_{34}) captures interaction between members 3 and 4, and local elastic follow-up (q_{12}) captures stress concentration effects. The component performance can be captured through maximum strain range and total elastic follow-up; however, measuring strain range and follow-up values at a point in a component during an experiment is not feasible. Therefore, conducting the SMT experiment with a specific strain range and elastic follow-up values is a challenging task.

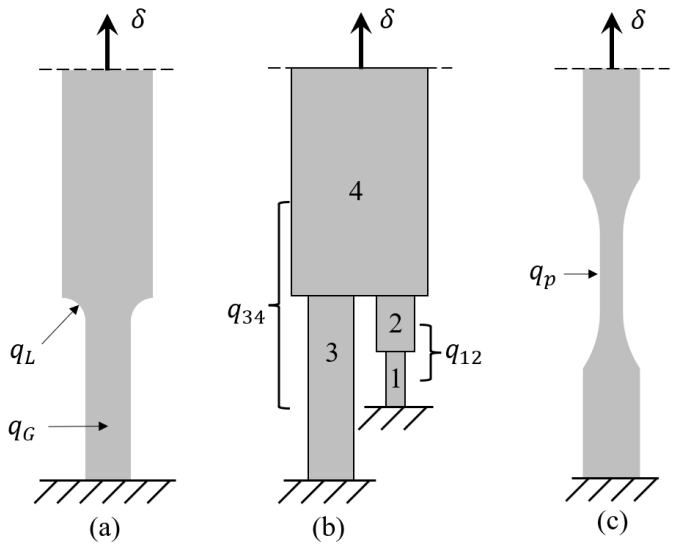

Figure 1. (a) Component showing global elastic follow-up q_n due to interaction of small and large bar and local elastic follow-up q_L due to stress raiser at the small and large bar connection, (b) representative four-bar problem (Jetter, 1998) capturing the local q_{12} and global q_{34} follow-ups in structure, and (c) SB-SMT specimen to capture the peak elastic follow-up q_p which bounds elastic follow-up values observed in component.

Work has been done to develop an SMT database for Alloy 617 in literature (Wang et al., 2015, Wang et al., 2016a, Wang et al., 2016b, Wang et al., 2018 Wang et al., 2019a, Wang et al., 2019b, Wang et al., 2021). Although component level SMT tests have shown success in capturing the desired strain range and follow-up values, these test specimens are large, and test setup requires a multiaxial loading system (Wang et al., 2015). The SMT experiment approach deals with a setup with the two bars with shared constraints. When displacement is applied to the two-bar system, the first bar remains elastic and second smaller bar experience stress relaxation with elastic follow-up. Due to the shared displacement compatibility, the first bar 'drives' the second bar (Wang et al., 2018). This approach has been used as proof of concept, and desired strain range and elastic follow-ups were achieved. This two-bar setup is a complex test procedure which limits the elastic follow-up values, as higher follow-ups demand excessively large driver dimensions, which may not be feasible to fabricate and test. Toward simplifying the test methodology, an SB-SMT has been developed (Wang et al. 2018). An electronic spring is introduced which controls strain by electronically amplifying the voltage of a strain signal to achieve different elastic follow-up factors (Wang et al., 2019b). The test results of the SB-SMT and the standard two-bar SMT are in agreement, indicating the success of the SB-SMT procedure (Wang et al., 2019a and Wang et al., 2019b). An alternate approach of SB-SMT was proposed through internal software controls, which control the test through software inputs and internal variables (McMurtrey and Simpson, 2020). This test requires 'virtual strain range' and dwell time as input. The 'virtual strain range' implicitly captures the desired follow-ups and actual strain range experienced by specimen. Due to the simplicity of the test inputs, software-controlled SB-SMT is a simple and efficient method that does not require hardware modification and is more readily applicable to general mechanical testing labs. Initial test results from software-controlled SB-SMT tests have been validated against the SB-SMT test conducted at ORNL (McMurtrey and Simpson, 2020). A proper methodology is needed to provide a step-by-step procedure for conducting software-controlled SB-SMT with a desired hold time and elastic follow-up factor.

This report presents the method to estimate test parameters for desired strain range and elastic follow-ups, a scoping test to validate estimated test parameter calculations, and test results obtained from the software-controlled SB-SMT. The Alloy 617 was selected as a candidate material, and all tests were conducted at 950℃. The test data serve as an addition to the existing SMT test database. The method to estimate and plan the SB-SMT is discussed, and recommendations will be used to develop the American Society for Testing and Materials (ASTM) standards for the SMT test.

3. SPECIMEN DETAILS

The SB-SMT tests were conducted on Alloy 617 with heat # 314626. The chemical composition of this heat is shown in Table 1. The geometry of the SB-SMT specimen geometry is presented in Figure 2. Note, this specimen is a typical elevated temperature fatigue ASTM specimen geometry. The standard ASTM specimen geometry is used for a SB-SMT experiment.

Table 1. Chemical composition of Alloy 617 (heat number 314626).

		Ni	Cr	Co	Mo	Fe	Mn	Al	C	Cu	Si	S	Ti	B
Heat 314626		54.1	22.2	11.6	8.6	1.6	0.1	1.1	0.05	0.04	0.1	<0.002	0.4	<0.001
ASME	Min	44.5	20.0	10.0	8.0			0.8	0.05					
	Max	-	24.0	15.0	10.0	3.0	1.0	1.5	0.15	0.5	1.0	0.015	0.6	0.006

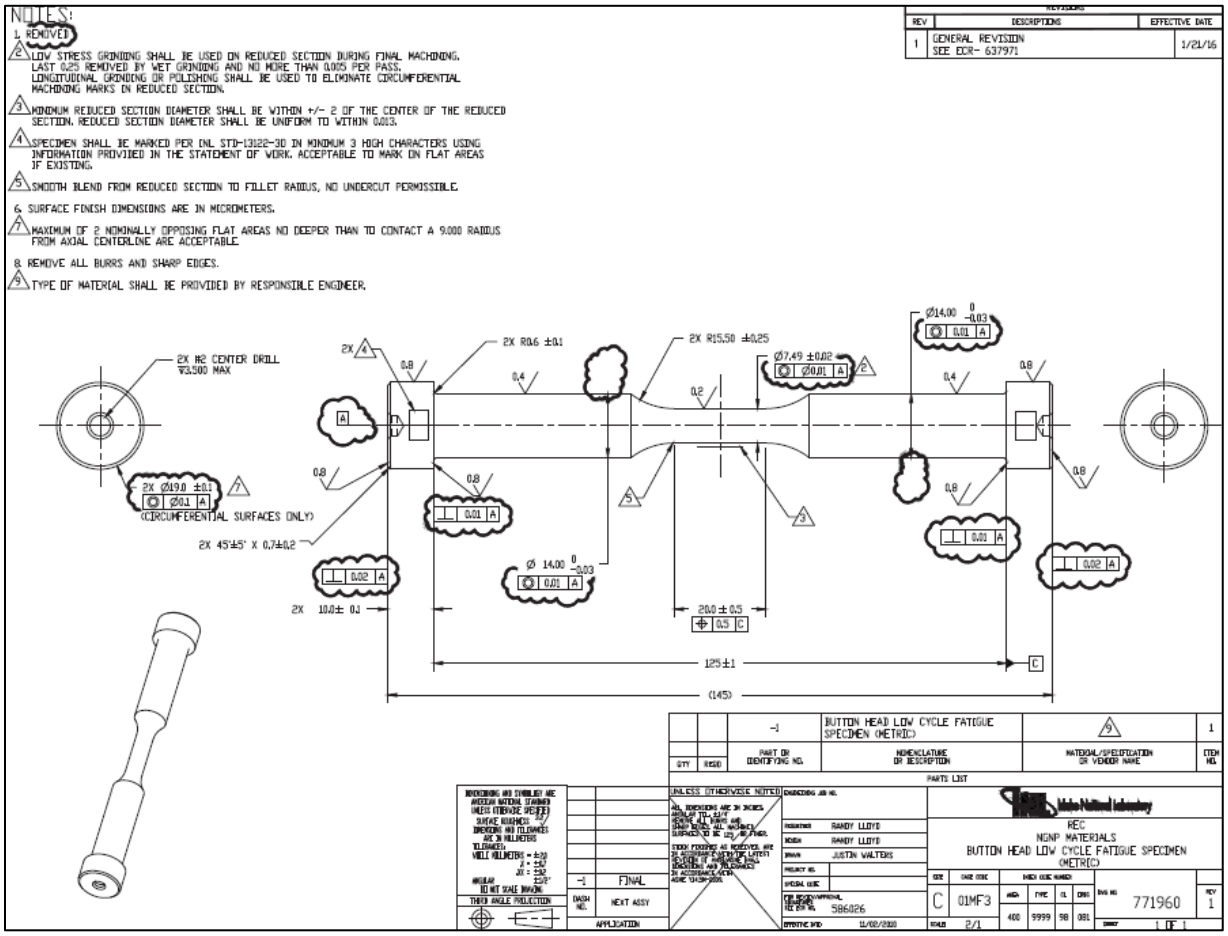

Figure 2. Specimen geometry used for SB-SMT tests.

4. TEST PROCEDURE

4.1 Introduction of Virtual Strain

SB-SMT follows a test procedure similar to the elevated temperature cyclic strain hold test. The SMT parameters are temperature, dwell time, follow-up value, strain range, and strain rate. The software-controlled SB-SMT requires additional parameters—elastic modulus at test temperature and 'virtual strain.' Elastic modulus of Alloy 617 can be determined either from the tension test or from Table TM-4 N-898, ASME BPVC, Section III, Division 5 (ASME, 2021). Previous work defined virtual strain as a function of the actual strain and the elastic follow-up as shown in Equation 1, where q is the elastic follow-up (McMurtrey and Simpson, 2020).

$$\varepsilon_v = \varepsilon + \frac{\sigma}{E}(q-1) \tag{1}$$

A typical strain-controlled strain dwell test results in stress relaxation during strain hold. The software-controlled SB-SMT procedure follows similar steps except strain is replaced by 'virtual strain.' The Blue curve in Figure 3a shows the software-controlled virtual strain, and the black curve represents the actual strain response recorded by an extensometer attached to the specimen. Virtual strain is held constant during dwell time. This results in relaxation in the material with a previously calculated follow-up value ensuring Equation 1 is always satisfied. The recorded stress-strain results in a desired elastic follow-up and strain range for the selected virtual strain range as shown in Figure 3b. The software controls the virtual strain internally and provides the desired follow-up and strain range results. This makes the software-controlled SB-SMT procedure a very efficient and easy way to conduct SMT experiments. The user needs to select the appropriate virtual strain range, elastic follow-up, and hold time for a given temperature to get desired results. By changing the virtual strain range input, the user could change the output results. Among the test parameter sets, selection of the virtual strain range is a critical step. At elevated temperature, material may experience cyclic softening or hardening, which may result in changes in the total strain range in SB-SMT. This material behavior makes the virtual strain range estimation for software-controlled SB-SMT a challenging task. At present, there is no methodology to estimate virtual strain range for desired actual strain range and elastic follow-up. The following subsection presents methods to address this issue and provides steps to calculate virtual strain range.

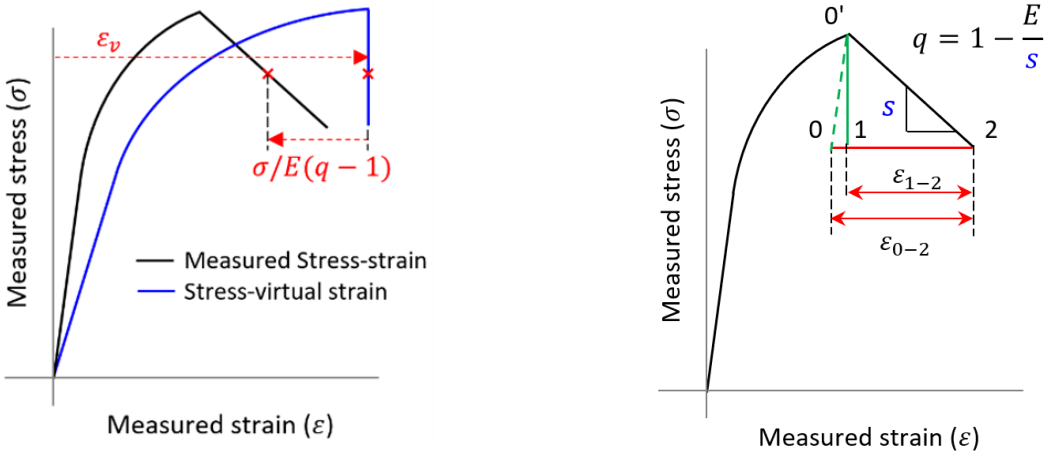

(a) (b)

Figure 3. Schematic representation of (a) stress-measured-strain against the stress-virtual-strain, and (b) the stress-strain curve obtained from typical SMT test with correlation of slope 's' and elastic follow-up value 'q'.

4.2 Virtual Strain Range Estimation

4.2.1 Detailed Calculations Through the Two-Bar Problem

A classical two-bar model was selected for the virtual strain range estimation. The classical two-bar model consists of two bars connected in series as shown in Figure 4. One end is fixed, and cyclic displacements are applied on the other end of this assembly. Stiffness ratios of two bars are selected such that the end displacement amplitude values are the same as the virtual strain amplitude values, and strain experienced by the small bar is identical to actual stress-strain experienced by the SMT specimen. End displacement (ε_v) is cycled and held constant at peak value for the desired dwell time. The Walker Alloy 617 material model available in the Nuclear Engineering Material model Library (NEML) simulated the material response. This material model is a viscoplastic constitutive model which can capture the kinematic and isotropic hardening, stress relaxation, and cyclic hardening or softening (Messner and Sham, 2021). Identical material is used for both bars. The area A_2 and length L_2 of the small bar is selected as one. The area of the large bar A_1 is selected as 1000. The length of the large bar L_1 is varied for different strain range and elastic follow-up values. The following equation relating the stiffnesses of the two bars and elastic follow-up was used (Wang et al., 2019b).

$$q = 1 + \frac{E_2 A_2}{L_2} \times \frac{L_1}{E_1 A_1} = 1 + \frac{L_1}{1000} \tag{2}$$

This equation estimated initial values of L_1. These values need to be slightly modified to get the accurate elastic follow-up and desired strain range in Bar 2 due to the influence of the material model. This step requires using the viscoplastic constitutive model with nonlinear analysis solvers. This method involves two iteration steps: (1) the first involves determination of accurate L_1 to get a desired elastic follow-up, and (2) the second iteration involves displacement amplitude ε_v to get the desired strain range for the given dwell time. Due to these two iterations and use of nonlinear constitutive model, this method is not a simple and efficient method. However, this method can provide the most accurate estimation of virtual strain range.

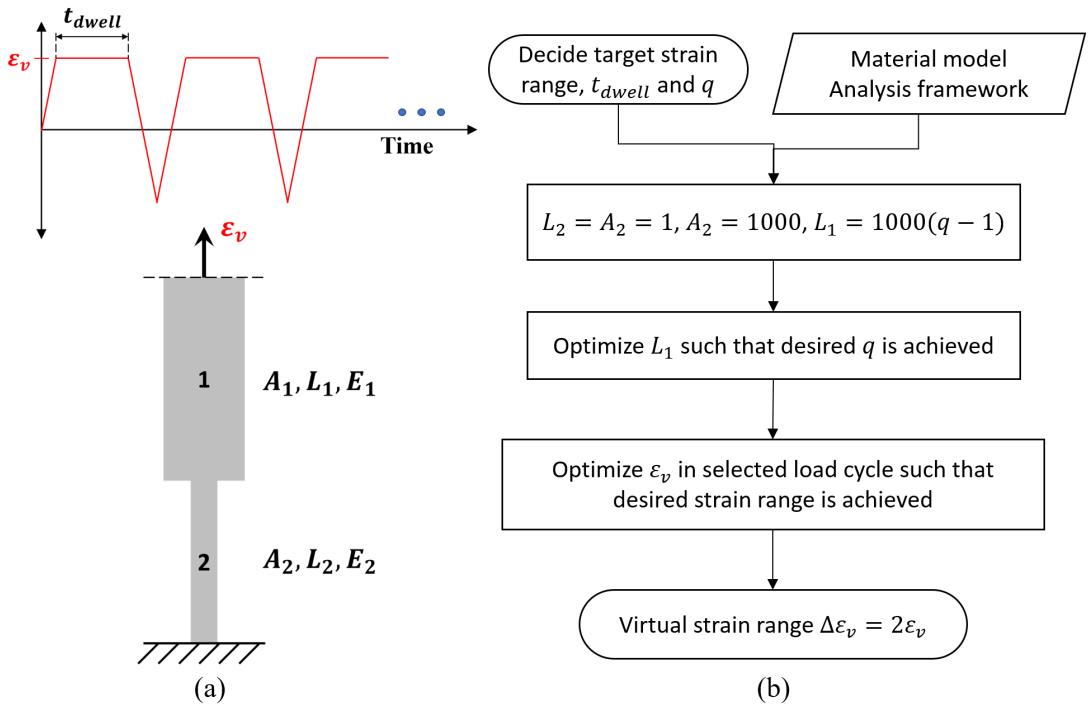

Figure 4. (a) Two-bar model with boundary conditions and adopted displacement history, and (b) flow chart used for virtual strain range estimation for two-bar problem.

4.2.2 Simplified Calculations

The goal is to estimate the total virtual strain range ($2\varepsilon_v$) such that the obtained total strain range matches with the target value. The flow chart of a virtual strain estimation process for a selected elastic follow-up, hold time, and anticipated total strain range shown in Figure 5. The following steps provide guidelines for virtual strain range estimation.

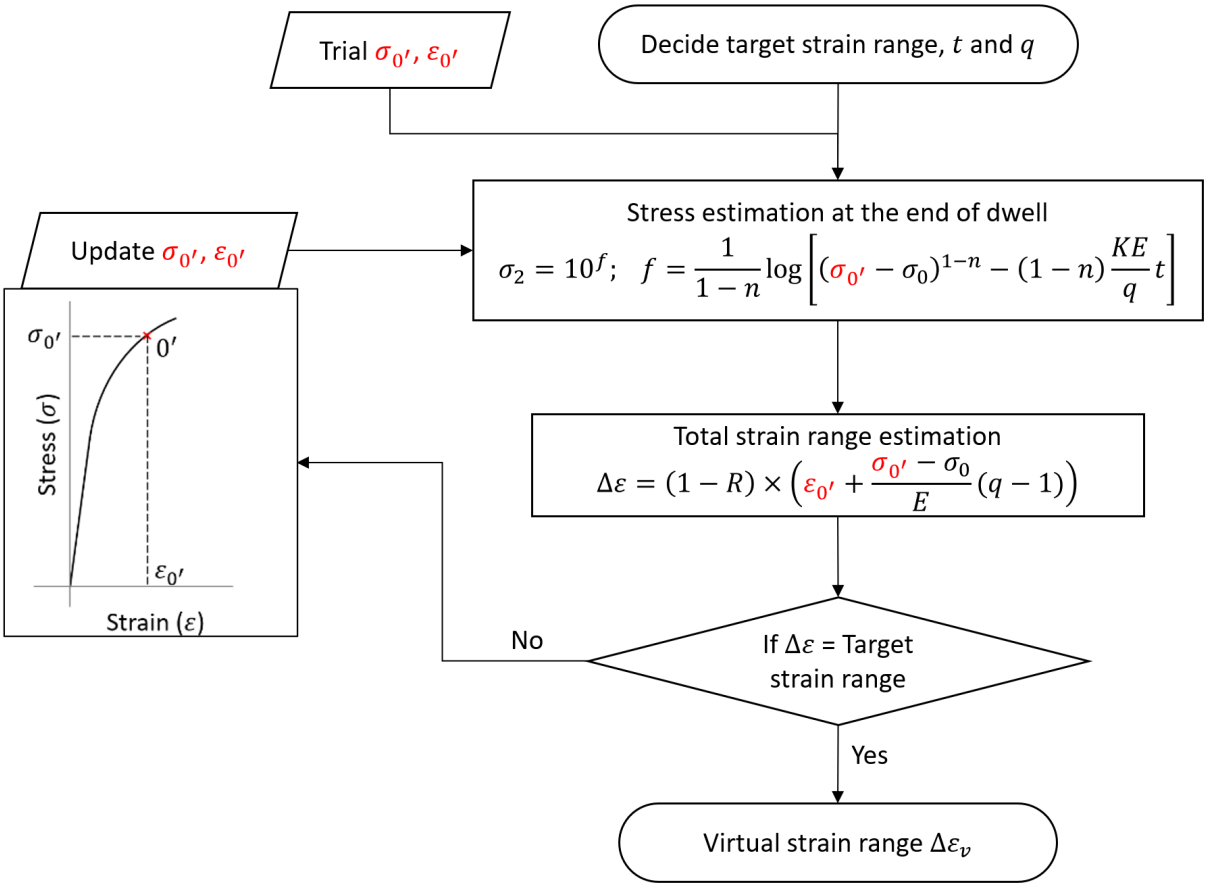

Figure 5. Flow chart for calculation of the virtual strain range to get the desired total strain range for selected elastic follow-up factor and dwell time.

1. **Decide test parameters**

Set stabilized strain range, elastic follow-up, hold time, and temperature. Select a trial stress $\sigma_{0'}$ and strain $\varepsilon_{0'}$ value at point $0'$ on the tension curve as shown in Figure 3b. This could either be obtained from a tension test, strain-controlled fatigue and creep-fatigue tests, or estimated from the hot tensile curve of the isochronous stress-strain curves (Figure HBB-T-1836 N-898, ASME BPVC Section III, Division 5) (ASME, 2021).

2. **Stress estimation at the end of dwell**:

The next step is to calculate the stress at end of the dwell time for the given elastic follow-up. The rate form of the Equation 1 is given as follows.

$$\dot{\varepsilon}_v = \dot{\varepsilon} + \frac{\dot{\sigma}}{E}(q-1) \tag{3}$$

During dwell, virtual strain is held constant, hence the virtual strain rate is zero. Total strain rate for a material can be decomposed into an elastic strain rate and an inelastic strain rate. An Elastic strain rate is given by Hook's law, and an inelastic strain rate is dominated by the stress relaxation which is calculated by using the Power law. Hence, Equation 3 is rewritten as,

$$0 = \frac{\dot{\sigma}}{E} + K\sigma^n + \frac{\dot{\sigma}}{E}(q-1) \tag{4}$$

Where, K and n are material parameters. These parameters are determined by fitting stress relaxation test results or from pure creep data setup with known stresses and minimum strain rates. Upon rearranging and integrating this equation from start of dwell time with peak stress $\sigma_{0'}$ to the end of dwell time t with stress relaxed to σ_2. This stress at the end of dwell is given as:

$$\sigma_2 = 10^f; \quad f = \frac{1}{1-n}\log\left[(\sigma_{0'} - \sigma_0)^{1-n} - (1-n)\frac{KE}{q}t\right] \tag{5}$$

3. **Total strain range estimation**:

This step calculates the actual strain range experienced by material as follows:

$$\Delta\varepsilon = (1 - R')\varepsilon_{0'} + \varepsilon_{1-2} \tag{6}$$

Where, R' is the ratio of actual strain experienced by material at the minimum and maximum stress. R' value depends on material properties, applied strain range, elastic follow-up, and dwell time. For large virtual strain range values R' approaches −1, for small strain range with high elastic follow-up R' would vary between −1 to 1. Hence, R' is bounded by [−1, <1]. Correct estimation of R' would require a large data set targeting multiple strain ranges with different elastic follow-up and dwell-time values. At present, limited data is available on the SMT specimen, so R' development from test data is not feasible.

The two-bar analysis framework discussed before generated a 'synthetic' data set. This data set was generated by using a wide set of strain ranges and elastic follow-ups with dwell times of 10 minutes, 1 hour, and 10 hours. Results of these analyses provided strain values $\varepsilon_{0'}$ and $\varepsilon_{-0'}$ from peak tension and compression stresses to calculate R' as shown in Figure 6a. The plot of calculated R' values against $\varepsilon_{0'}$ in Figure 6b shows R' starts with −1. With an increase in strain this number increases as much as 0.2. Beyond this point, R' values start decreasing and stabilize to −1 for higher strain values for all elastic follow-up values. This data set was developed with the Walker's constitutive model available in NEML, which captures the complex cyclic time- and temperature-dependent material behavior (Messner and Sham, 2021). Thus, this viscoplastic constitutive model captures the complex creep-fatigue interaction of material at elevated temperature with reasonable accuracy. Hence, the developed synthetic data set represents actual material behavior. Ratcheting is observed in material under SMT load cycle, and Alloy 617 at elevated temperature shows strain range dependent hardening which explains the significant change in R' values. This data set was used to develop empirical relations between R' and $\varepsilon_{0'}$. Equation 7 correlates R' for the trial strain value $\varepsilon_{0'}$. This equation uses two linear equations to capture the increasing and decreasing nature of R', and this value is bounded by −1. Note that for other hold cases such as compression hold or combination of compression and tension hold, this bound is not applicable. Parameters m_1, m_2, c_1, and c_2 are calculated as a function of elastic follow-up using Equation 8.

$$R' = \max\begin{cases}\dfrac{\min([m_1\varepsilon_{0'} + c_1], [m_2\varepsilon_{0'} + c_2])}{\varepsilon_{0'}} \\ -1\end{cases} \tag{7}$$

$$\begin{aligned} m_1 &= m_{12}q^2 + m_{11}q + m_{10}, \qquad m_2 = m_{22}q^2 + m_{21}q + m_{20} \\ c_1 &= c_{12}q^2 + c_{11}q + c_{10}, \qquad c_2 = c_{22}q^2 + c_{21}q + c_{20} \end{aligned} \tag{8}$$

Where, m_{ij} and c_{ij} are fitting parameters and values are provided in Table 2.

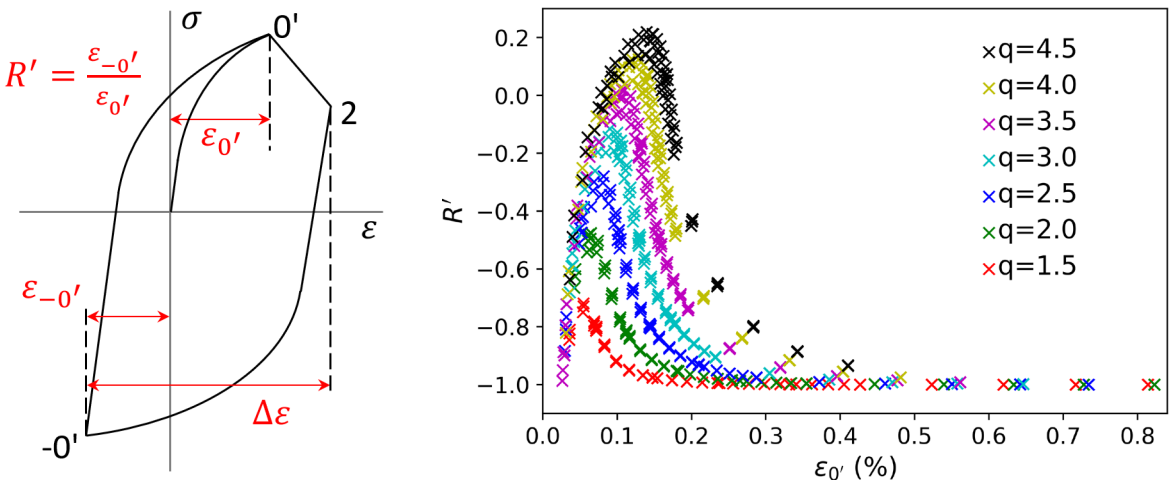

(a) (b)

Figure 6. (a) Schematic figure showing stress-strain hysteresis loop of the SMT and R' calculation, and (b) plot of R' values against the trial strain $\varepsilon_{0'}$ at point $0'$ calculated for different elastic follow-up values and dwell time from two-bar problem analysis framework.

Table 2. Parameter set used to calculate m_1, m_2, c_1, and c_2 to estimate R'.

	A_{i2}	A_{i1}	A_{i0}
m_{1j}	−0.071078	0.66854	−1.1630
m_{2j}	−0.015610	0.37267	−1.2746
c_{1j}	0.001777	−0.016713	0.004075
c_{2j}	0.039025	−0.093168	0.068657

The equations discussed above were used to predict R' values for different strain and elastic follow-up. These values were compared against the 'synthetic' data in Figure 7. This comparison shows the linear empirical equation reasonably captures the complex interaction of R' values for different strain and elastic follow-up. Hence, above equations are used to calculated R' value to estimate the total actual strain range.

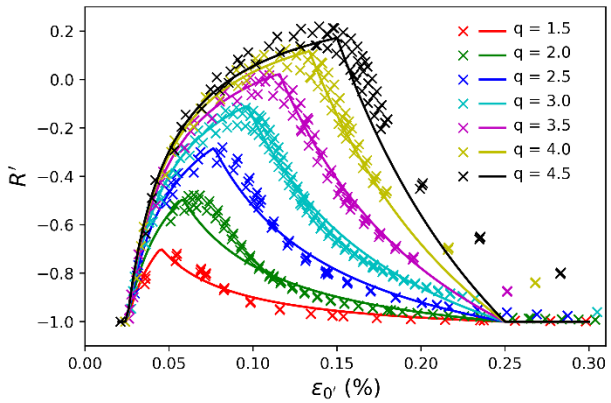

Figure 7. Comparison of estimated R' based on empirical equations shown in solid lines against calculated R' values from the two-bar analysis shown in cross points for different elastic follow-ups.

The elastic follow-up equation is rewritten as follows:

$$q = \frac{\sigma_{0'-2} + E\varepsilon_{1-2}}{\sigma_{0'-2}} \tag{9}$$

$$\varepsilon_{1-2} = \frac{\sigma_{0'} - \sigma_2}{E}(q-1) \tag{10}$$

Insert this strain and stress at the end of hold from Equation 10 in Equation 6.

$$\Delta\varepsilon = (1-R')\varepsilon_{0'} + \frac{\sigma_{0'} - \sigma_2}{E}(q-1) \tag{11}$$

If the calculated actual strain range $\Delta\varepsilon$ is smaller than the target actual strain range, then the point $0'$ with higher trial stress-strain is selected, else vice versa. These trial stress-strain points are used as input in the Step 2, and process is repeated until the target strain range is reached. Once $\Delta\varepsilon$ matches the target strain range, the virtual strains are calculated.

4. **Virtual strain range**:

Calculate the respective virtual strain range using following equation.

$$\Delta\varepsilon_v = 2\left[\varepsilon_2 + \frac{\sigma_2}{E}(q-1)\right] \tag{12}$$

This virtual strain range estimation procedure is simple but depends on several assumptions. The most critical assumption is selection of correct value R'. This method also assumes that during dwell time, creep deformations are the only governing deformation mechanism. Due to these assumptions, the proposed virtual strain range estimation method needs validation through SMT experiment.

5. RESULTS AND DISCUSSION

5.1 Scoping Test

To validate the proposed virtual strain range estimation techniques, a scoping test was conducted with a series of strain range, elastic follow-ups, and dwell times. Few cycles were applied to capture the strain range and elastic follow-up, and the test data was used as a validation for the proposed estimation methods. Table 3 presents the scoping test parameters, observed strain ranges and elastic follow-ups, and simulated strain ranges from two methods discussed in the previous section. The simulated strain range values based on selected virtual strain ranges from two different methods compares well with the observed experimental strain ranges. The simulated hysteresis stress-strain loops obtained from the two-bar analysis framework are compared against the experimental hysteresis loops for different SB-SMT load cycles in Figure 8a–p which show the desired elastic follow-up and strain range was achieved in scoping SB-SMT test. Note that viscoplastic constitutive model parameters were determined from a wide set of experiments from different heats (Messner and Sham, 2021). The model captures average material response such as strain range, ratcheting rates, and stress relaxation time history during elastic follow-up with higher accuracy. The actual stress-strain amplitude of material may differ based on material heat and local chemistry of specimen which leads to difference between simulated and experimental hysteresis loop as shown in Figure 8a-p.

Table 3. Test details for a scoping test at 950℃ presenting a series of load cycles to be applied on the specimen with calculated virtual strain range, L_1/L_2 ratio used for two-bar calculations, calculated strain range ($\Delta\varepsilon$) from simplified calculation method and from two-bar calculation method, the observed strain range and follow-up values (q) in test data [t_{dwell} = dwell time, $\Delta\varepsilon_v$ = end displacement].

Load cycle name	**Test parameters**				**Scoping test results**		**Simplified calculation of $\Delta\varepsilon$ (%)**	**Two-bar calculation**	
	t_{dwell} (min)	**Cycles**	**$\Delta\varepsilon_v$ (%)**	**q**	**$\Delta\varepsilon$ (%)**	**q**		**$\frac{L_1}{L_2}$**	**$\Delta\varepsilon$ (%)**
48-3 test 1	10	5	0.306	2	0.1687	2.04	0.1811	1065	0.1828
48-3 test 1-1	10	5	0.306	2	0.1773	2.01	0.1811	1065	0.1828
48-3 test 4	10	5	0.386	3	0.1400	3.02	0.1633	2131	0.1518
48-3 test 8	10	5	0.506	3	0.2238	3.01	0.2189	2131	0.2391
48-3 test 9	600	5	0.478	3	0.2165	3.02	0.2244	2131	0.2370
48-3 test 10	10	3	0.400	3	0.1470	3.00	0.1696	2131	0.1604
48-3 test 11	10	3	0.400	2	0.2673	2.00	0.2551	1065	0.2677
48-3 test 12	10	5	0.662	4.5	0.1902	4.44	0.2474	3735	0.2027
48-3 test 13	10	5	0.510	2	0.3826	2.03	0.3463	1065	0.3735
48-3 test 14	10	5	0.710	2.23	0.5500	2.19	0.5116	1310	0.5379
48-3-EP-1	10	5	0.308	3	0.1156	3.01	0.1271	2131	0.1120
48-3-EP-2	10	5	0.414	3	0.1611	3.06	0.1764	2131	0.1694
48-3-EP-3	10	5	0.562	3	0.2835	3.01	0.2447	2131	0.2876
48-3-EP-4	10	5	0.626	3	0.3552	2.98	0.2894	2131	0.3464
48-3-q2-ft	60	5	0.406	2	0.2809	2.00	0.2649	1065	0.2793
48-3-q3-ft	60	5	0.496	3	0.2274	3.03	0.2258	2131	0.2412

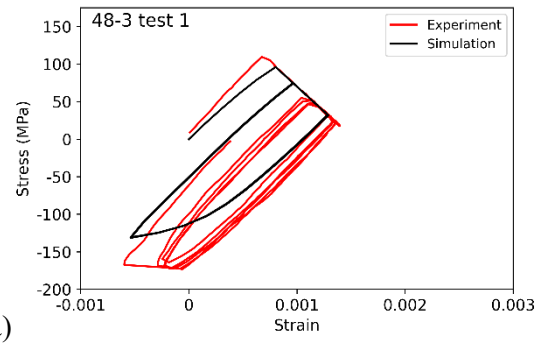
48-3 test 1
Experiment
Simulation
Stress (MPa)
Strain

(a)

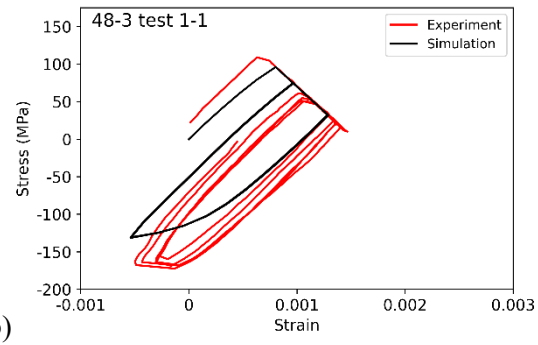
48-3 test 1-1
Experiment
Simulation
Stress (MPa)
Strain

(b)

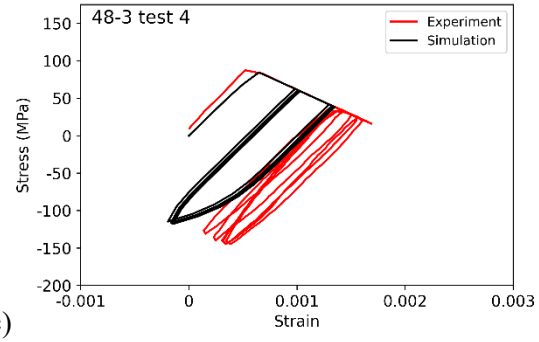
48-3 test 4
Experiment
Simulation
Stress (MPa)
Strain

(c)

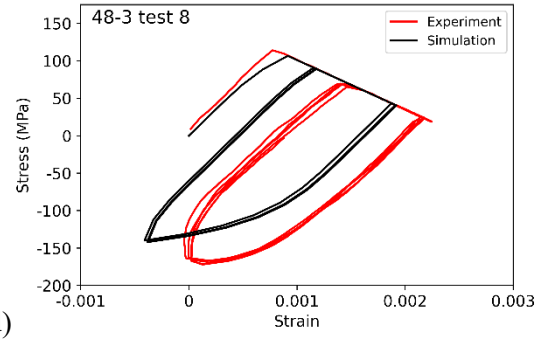
48-3 test 8
Experiment
Simulation
Stress (MPa)
Strain

(d)

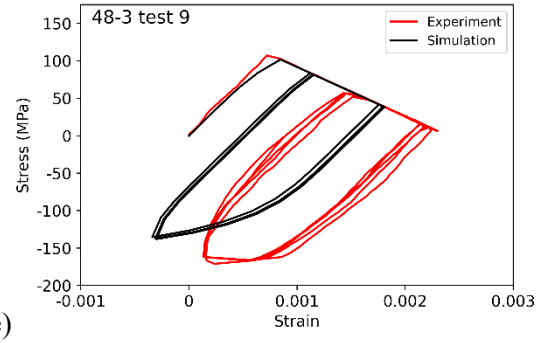
48-3 test 9
Experiment
Simulation
Stress (MPa)
Strain

(e)

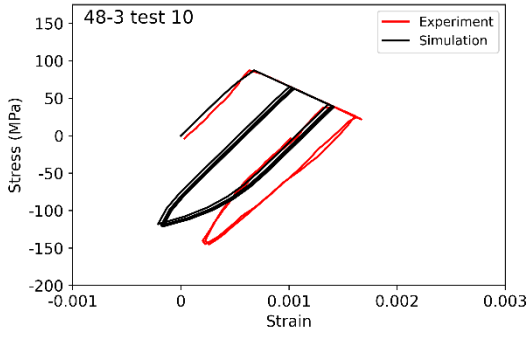
48-3 test 10
Experiment
Simulation
Stress (MPa)
Strain

(f)

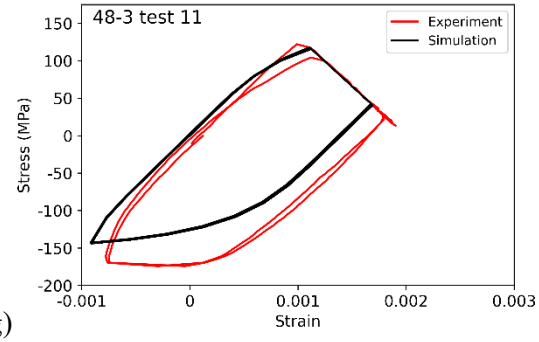
48-3 test 11
Experiment
Simulation
Stress (MPa)
Strain

(g)

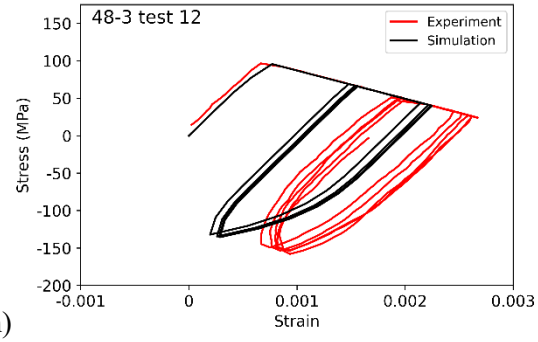
48-3 test 12
Experiment
Simulation
Stress (MPa)
Strain

(h)

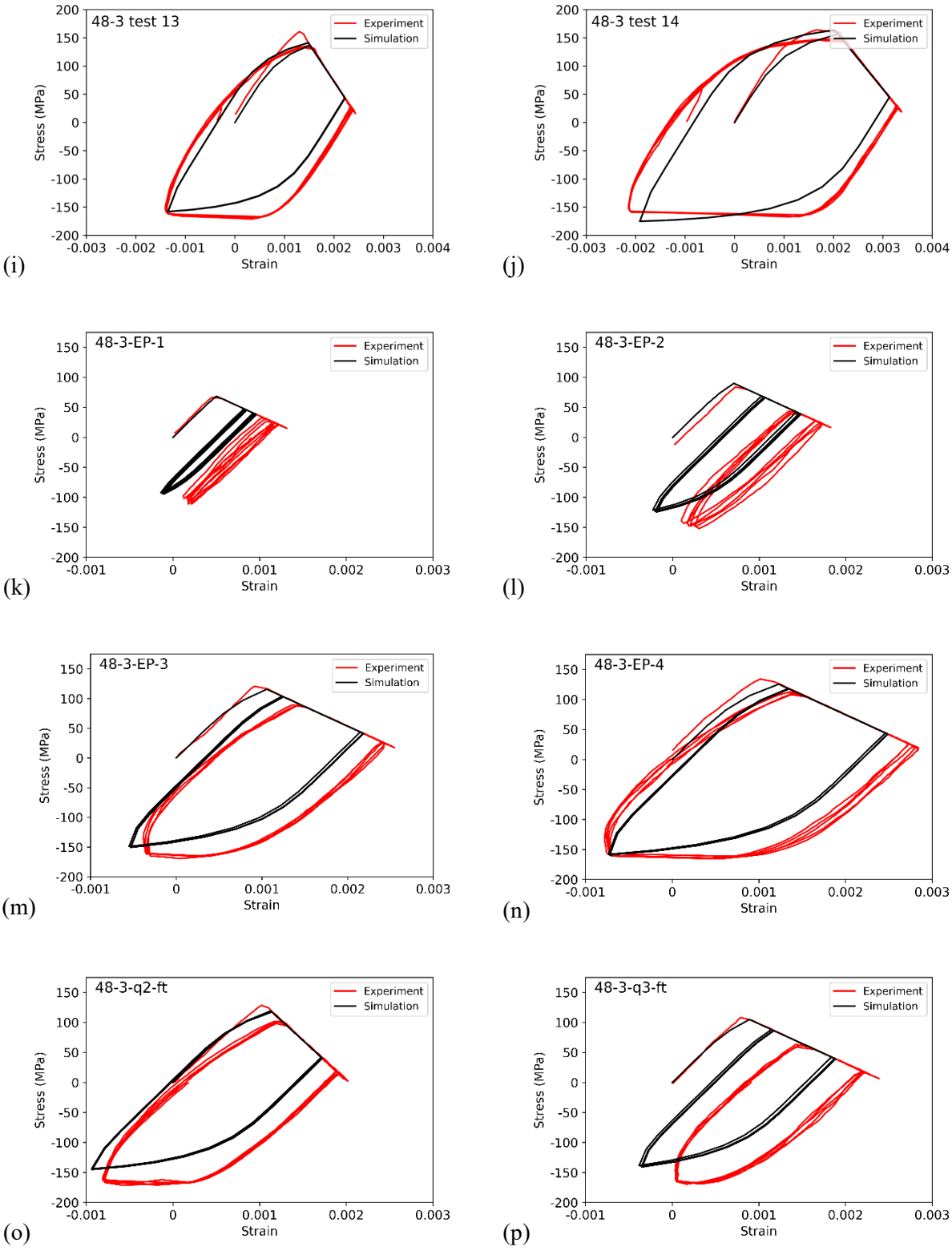

Figure 8. Comparison of the observed stress-strain hysteresis loops from the scoping test conducted on 48-3 specimen against the simulated stress-strain curves from the two-bar problem.

5.2 SB-SMT Test

The virtual strain range was calculated and used to conduct an SB-SMT test. The test number 48-4 was started with elastic follow-up of 3, dwell time at tensile hold of 10 minutes, and target strain range of 0.2%. The first, 100th and stabilized cycle's hysteresis loops and stress relaxation histories are plotted in Figure 9. The hysteresis loop plots in Figure 9a shows the target elastic follow-up was achieved. Stress relaxation history shows reduction in peak stresses and stresses at the end of dwell with increase in cycles.

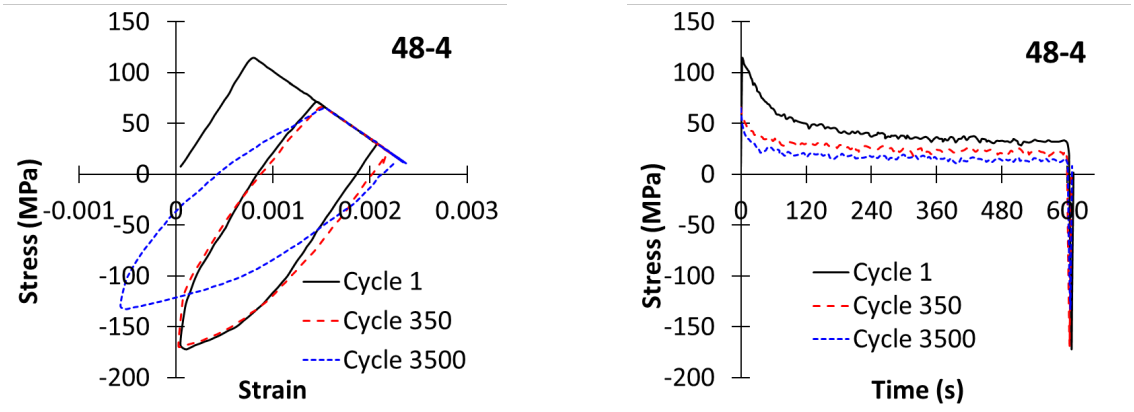

(a) (b)

Figure 9. SB-SMT test results showing (a) Hysteresis stress-strain curves and (b) Stress relaxation time history recorded at different cycles.

The ratio of peak tensile to compressive stresses (R) against cycle number and strain range evolution recorded by an extensometer against cycles are presented in Figure 10. This figure shows a typical ratcheting-type behavior commonly observed in SMT experiments. Due to ratcheting effects, actual strain range increase is observed in the specimen. The specimen ruptured at 4522th cycle following a 20% drop in ratio 'R' method (Totemeier and Tian, 2007).

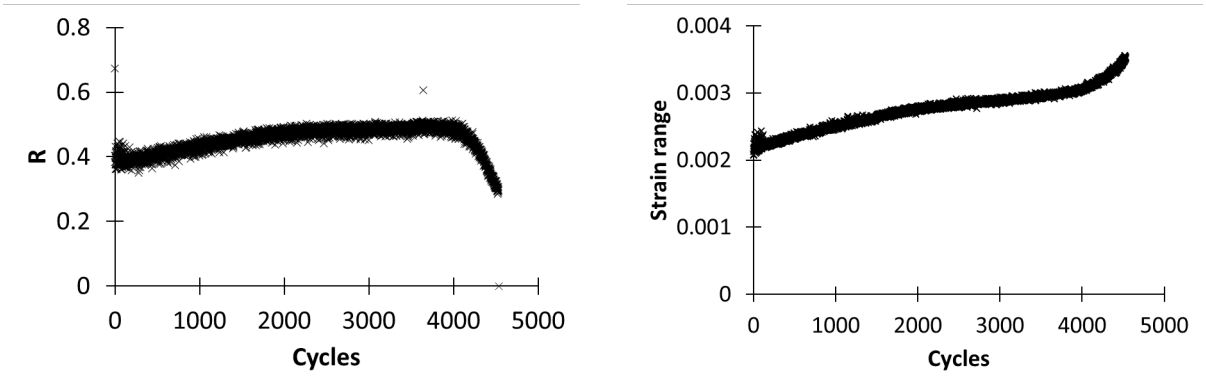

(a) (b)

Figure 10. SB-SMT test results showing (a) ratio of peak tensile and compressive stresses (R) against cycle count and (b) strain range evolution against cycle count.

6. CONCLUSION AND ONGOING WORK

This report presents analytical methods to estimate the virtual strain range required for software-controlled SB-SMT experiment. These analytical methods are validated through a scoping software-controlled SB-SMT covering a wider strain range, elastic follow-ups, and dwell time. The proposed virtual strain range estimation method achieves target strain range, and validates the software-controlled SB-SMT procedure and virtual strain range estimation method. A test plan was developed with respective calculated virtual strain ranges to be performed on Alloy 617.

At present, a software-controlled SB-SMT experiment test plan is in progress following the test plan per Table 4. These test results will improve the current SMT data set for Alloy 617. Coupled creep-fatigue damage will be calculated and compared against the current SMT design curve either to justify or to improve the proposed SMT design curves.

Table 4. Test plan of SB-SMT to be performed on Alloy 617 with strain range of 0.2% at 950℃.

Follow-up	Hold (min)	Strain rate (1/sec)
3 (Test finished)	10	0.001
3	30	0.001
3	60	0.001
2	10	0.001
2	30	0.001
2	60	0.001
3	600	0.001
3	10	0.0001
3	10	0.00001

7. REFERENCES

ASME. (2021). Boiler and Pressure Vessel Code. New York, NY: ASME.

Barua, B., Messner, M.C., Sham, T.L., Jetter, R.I. and Wang, Y., 2020. Preliminary description of a new creep-fatigue design method that reduces over conservatism and simplifies the high temperature design process (No. ANL-ART-194). Argonne National Lab. (ANL), Argonne, IL (United States).

Barua, B., Messner, M.C., Wang, Y., Sham, T.L. and Jetter, R.I., 2021. Draft Rules for Alloy 617 Creep-Fatigue Design using an EPP+SMT Approach (No. ANL-ART-227). Argonne National Lab. (ANL), Argonne, IL (United States).

Jetter, R.I., 1998. An Alternate Approach to Evaluation of Creep-Fatigue Damage for High Temperature Structural Design Criteria. ASME-PUBLICATIONS-PVP, 365, pp.199-206.

Jetter, R.I., Sham, T.L. and Wang, Y., 2016. FY16 Status Report on Development of Integrated EPP and SMT Design Methods (No. ANL-ART-53). Argonne National Laboratory (ANL), Argonne, IL (United States).

McMurtrey, M.D. and Simpson, J.A., 2020. Single-Bar SMT Testing on Alloy 617 using Software Controls (No. INL/EXT-20-59163-Rev000). Idaho National Laboratory (INL), Idaho Falls, ID (United States).

Messner, M. C., and Sham, T. -L. 2021. "Reference constitutive model for Alloy 617 and 316H stainless steel for use with the ASME Division 5 design by inelastic analysis rules". United States. https://doi.org/10.2172/1818970. https://www.osti.gov/servlets/purl/1818970.

R Roche., 1981, Appraisal of Elastic Follow Up. International Conference on Structural Mechanics in Reactor Technology.

Totemeier, T.C. and Tian, H., 2007. Creep-fatigue–environment interactions in INCONEL 617. Materials Science and Engineering: A, 468, pp.81-87.

Wang, Y., Jetter, R.I., Baird, S.T., Pu, C. and Sham, T.L., 2015. Report on FY15 Alloy 617 SMT Creep-Fatigue Test Results. ORNL/TM-2015/300, Oak Ridge National Laboratory, Oak Ridge, TN.

Wang, Y., Jetter, R.I. and Sham, T.L., 2016a. Preliminary Test Results in Support of Integrated EPP and SMT Design Methods Development. ORNL/TM-2016/76, Oak Ridge National Laboratory, Oak Ridge, TN.

Wang, Y., Jetter, R.I. and Sham, T.L., 2016b. FY16 Progress Report on Test Results in Support Of Integrated EPP and SMT Design Methods Development. ORNL/TM-2016/330, Oak Ridge National Laboratory, Oak Ridge, TN.

Wang, Y., Jetter, R.I., Messner, Mark C. and Sham, T.L. 2018. Report on FY18 Testing Results in Support of Integrated EPP-SMT Design Methods Development (No. ORNL/TM-2018/887). Oak Ridge National Laboratory (ORNL), Oak Ridge, TN (United States).

Wang, Y., Jetter, R.I., Messner, M.C. and Sham, S., 2019a. Report on FY19 Testing in Support of Integrated EPP-SMT Design Methods Development (No. ORNL/TM-2019/1224). Oak Ridge National Laboratory (ORNL), Oak Ridge, TN (United States).

Wang, Y., Jetter, B. and Sham, T.L., 2019b, July. Effect of Internal Pressurization on the Creep-Fatigue Performance of Alloy 617 Based on Simplified Model Test Method. In Pressure Vessels and Piping Conference (Vol. 58929, p. V001T01A066). American Society of Mechanical Engineers.

Wang, Y., Hou, P., Messner, M.C., Jetter, R.I. and Sham, T.L., 2021. Testing in Support of the Development of EPP Plus SMT Design Method at ORNL (FY2021) (No. ORNL/TM-2021/2159).